ACS APPLIED MATERIALS & INTERFACES

Research Article

www.acsami.org

Three-Dimensional Fe(II)-based Metallo-Supramolecular Polymers with Electrochromic Properties of Quick Switching, Large Contrast, and High Coloration Efficiency

Chih-Wei Hu,[†] Takashi Sato,[‡,§] Jian Zhang,[‡,§] Satoshi Moriyama,[†,§] and Masayoshi Higuchi*[,‡,§]

[†]International Center for Materials Nanoarchitectonics (MANA), National Institute for Materials Science (NIMS), 1-1 Namiki, Tsukuba 305-0044, Japan

[‡]Electronic Functional Materials Group, Polymer Materials Unit, National Institute for Materials Science (NIMS), 1-1 Namiki, Tsukuba 305-0044, Japan

[§]JST-CREST, Tokyo 102-0076, Japan

Supporting Information

ABSTRACT: A series of Fe(II)-based metallo-supramolecular polymers with three-dimensional (3-D) structures were synthesized by the stepwise complexation of an Fe(II) salt with different ratios of a linear bis(terpyridine) ligand and a branched tris(terpyridine) ligand. Atomic force microscopy images of the polymer films showed a drastic change in the surface morphology upon varying the amount of the branched ligand. The surface of a designed 3-D construction film showed a highly porous structure (pore size: approximately 30−50 nm in diameter), probably due to the formation of a hyperbranched polymer structure. All the 3-D polymers had a blue color based on the metal-to-ligand charge-transfer (MLCT) absorption and exhibited excellent electrochromic properties. The most highly porous 3-D-structured film showed the best electrochromic performance; as compared with a 1-D linear polymer, the switching times were improved 38.7% for the coloring (0.31 → 0.19 s) and 37.9% for the bleaching (0.58 → 0.36 s). The transmittance change (ΔT) increased 21.8% (41.6 → 50.7%). Also, the coloration efficiency (η) was enhanced 45.3% (263.8 → 383.4 $cm^2\ C^{-1}$). The redox in the 3-D film was diffusion-controlled, as supported by the linear relationship between the current and square root of the scan rate. It is considered that the porous structure of the 3-D polymer films contributed to smooth ionic transfer during the redox and to the improved electrochromic properties.

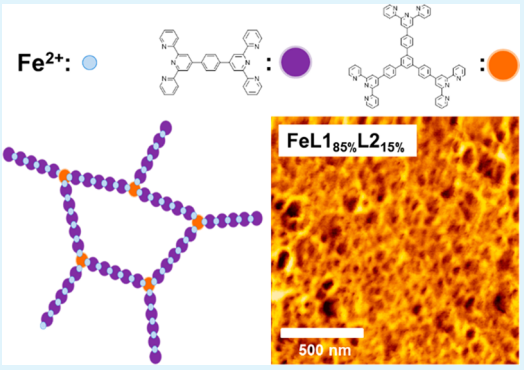

KEYWORDS: *coloration efficiency, electrochromism, metallo-supramolecular polymer, 3-D, self-assembly*

INTRODUCTION

Since Deb reported an electrochromic device in 1969,[1] new electrochromic materials (ECMs) have been found/investigated. For the widely studied ECMs, the first-generation materials were metal oxides;[2,3] the second, transition metal complexes;[4−7] the third, organic molecules and conducting polymers;[8−11] the fourth, metallo-supramolecular polymers.[12−18] The first- to third-generation ECMs have greatly contributed to the development of both fundamental properties and display applications, such as smart windows. Fourth-generation metallo-supramolecular polymers are a new type of ECM synthesized by the 1:1 complexation of transition metal ions such as Fe(II) and Ru(II) ions and ditopic organic ligands. The polymers have a one-dimensional (1-D) linear structure and show reversible electrochromic behavior based on the appearance/disappearance of the metal-to-ligand charge-transfer (MLCT) absorption, which is triggered by the electrochemical redox of the metal ions. Red-, green-, and blue-colored polymers have been prepared using Ru(II), Cu(II), and Fe(II) ions, respectively, according to the different band gaps of the MLCT absorption.[19,20] The multicolor electrochromic (EC) behavior has also been achieved by the introduction of two metal ion species to the polymer chains as a result of the different redox potentials of the metal ions.[21]

In the past decade, studies have shown that the structure significantly affects the EC properties in first- to third-generation ECMs.[22−30] It is thus expected that the EC properties of metallo-supramolecular polymer films are also influenced by the morphology, but there are no reports regarding the relationship between the morphology of metallo-supramolecular polymer films and their EC properties. The introduction of a three-dimensional (3-D) structure to the metallo-supramolecular polymer backbone is anticipated to affect the surface morphology, solubility, intrafacial and/or interfacial electron transfer speed, maximum absorption wavelength, and thermal properties. As for the 3-D polymer,

Received: February 23, 2014
Accepted: May 19, 2014
Published: May 19, 2014

   dx.doi.org/10.1021/am5010859 | ACS Appl. Mater. Interfaces 2014, 6, 9118−9125

Scheme 1. Synthesis of the 3-D Metallo-Supramolecular Polymers ($FeL1_{x\%}L2_{y\%}$)

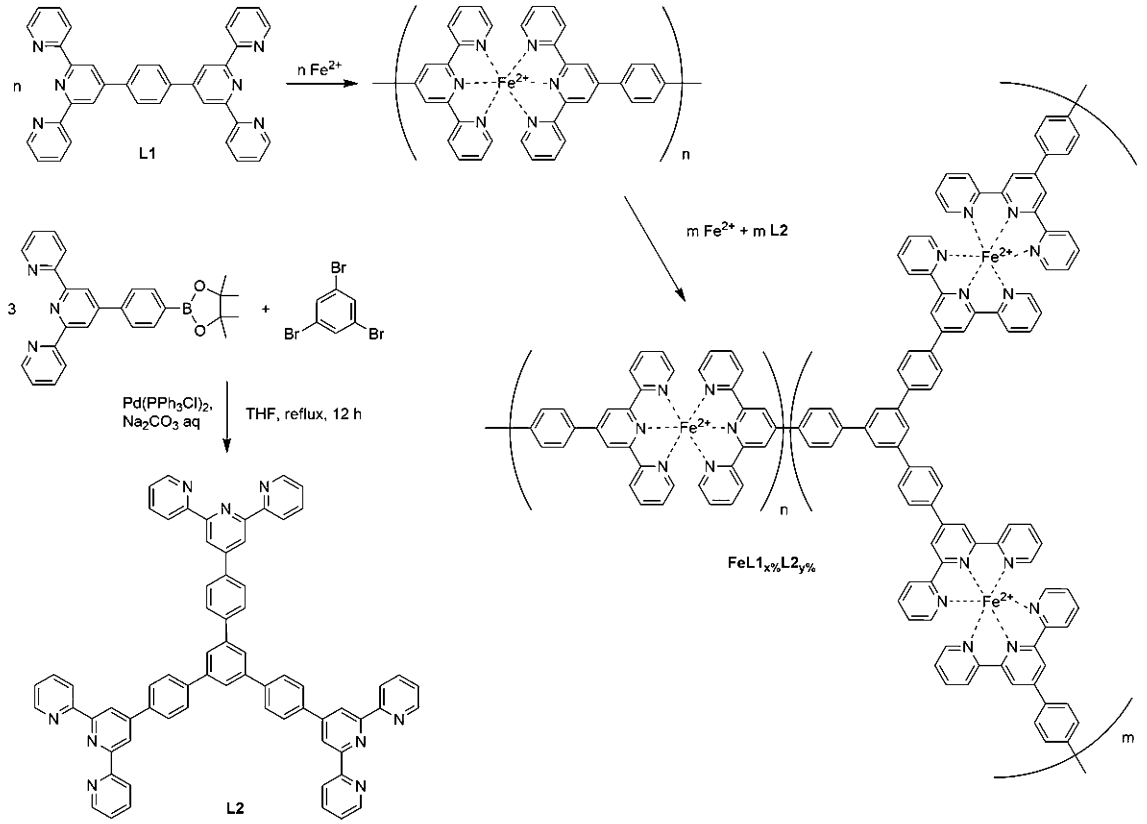

Kurth and his co-workers combined bis(terpyridine) and tris(terpyridine) ligands to form cross-linked metallo-supramolecular coordination polyelectrolytes (MEPEs), and they revealed the effect of the cross-linking on the solubility; however, they did not show the effect on the optical and electrochromic properties of the polyelectrolytes.[31] Tieke and his co-workers reported that polymer complexes with pendant terpyridine moieties as trapping sites for Zn(II) ions showed fast EC response and multiple color changes by using different anions,[32−34] but the polymer films were fabricated by a layer-by-layer method; they did not show the cross-linked properties of site-chain-linked polymers. Here we report the relationship between the 3-D structure and the EC properties in metallo-supramolecular polymer films for the first time.

Fe(II)-based metallo-supramolecular polymers with a 3-D structure ($\mathbf{FeL1_{95\%}L2_{5\%}}$, $\mathbf{FeL1_{90\%}L2_{10\%}}$, $\mathbf{FeL1_{85\%}L2_{15\%}}$, $\mathbf{FeL1_{82\%}L2_{18\%}}$, $\mathbf{FeL1_{80\%}L2_{20\%}}$) and a 1-D linear structure ($\mathbf{FeL1_{100\%}}$) were synthesized by the stepwise complexation of an Fe(II) salt with different ratios of bis(terpyridine) (**L1**) and tris(terpyridine) (**L2**)[35] (Scheme 1). First, the 1-D polymer chains were prepared by the 1:1 complexation of Fe^{2+} and **L1**, and then **L2** and Fe^{2+} were added to the solution to make a 3-D structure. The successive addition should first lead to linear polymers, followed by formation of highly cross-linked polymers. The degree of branching was controlled by changing the molar ratio of **L1** and **L2** from 95:5 to 80:20. In the report by Kurth et al.,[31] the three components (a metal ion, a ditopic ligand, and a tritopic ligand) are mixed at the same time in order to synthesize 3-D polymers; however, we added the two ligands (**L1** and **L2**) in turn. As the result, the length of the linear parts in the 3-D polymers would be more uniform because **L2** connects the formed 1-D polymer chains three-dimensionally.

EXPERIMENTAL SECTION

Chemicals and Instruments. All chemicals were reagent grade and used without purification. Methanol (MeOH) and acetic acid (AA) were used as reaction solvents. The acetonitrile (ACN) used for UV−vis and cyclic voltammetry (CV) measurements was spectrochemical analysis grade. These solvents were purchased from Wako, Aldrich, or Kanto Chemical Co. Inc. and used as received. The melting point was observed using an MP50 melting-point system from Mettler Toledo (temperature range: room temperature to 300 °C). ^{1}H-NMR spectra were recorded at 300 MHz on a JEOL AL 300/BZ instrument. Chemical shifts were given relative to tetramethylsilane (TMS). Mass spectra (MS) were measured by using AXIMA-CFR, a Shimadzu/Kratos time-of-flight (TOF) mass spectrometer. The UV−vis spectra were obtained with a Shimadzu UV-2550 UV−visible spectrophotometer. The 4′,4′′′′-(1,4-phenylene)bis(2,2′:6′,2″-terpyridine) (**L1**) was purchased from Aldrich (97%) and used without further purification. Iron(II) acetate [$Fe(OAc)_2$, >99.99%] was purchased from Aldrich. The supporting electrolytes, lithium perchlorate ($LiClO_4$, 99%), tetrabutylammonium perchlorate (TBAP, 98%), and silver nitrate ($AgNO_3$, 99%) were purchased from Aldrich and used without further purification. CV and amperometric experiments were conducted in an argon-saturated anhydrous acetonitrile solution containing 0.1 M $LiClO_4$ as a supporting electrolyte using an electrochemical analyzer. A platinum wire was used as the counter electrode, and a homemade Ag/Ag^+ electrode in ACN with 0.1 M TBAP + 0.01 M $AgNO_3$ as the reference.

Synthesis of L2.[35] After a mixture of 4′-(4-(4,4,5,5-tetramethyl-1,3,2-dioxaborolan-2-yl)phenyl)-2,2′:6′,2″- terpyridine (1.74 g, 4.00 mmol), 1,3,5-tribromobenzene (315 mg, 1.00 mmol), $Pd(PPh_3)_4$ (116 mg, 0.1 mmol), 0.2 M aqueous Na_2CO_3 (30 mL, 6.00 mmol), and THF (210 mL) was refluxed for 12 h, the precipitate was isolated by filtration, washed with tetrahydrofuran (THF), water, and finally

dx.doi.org/10.1021/am5010859 | ACS Appl. Mater. Interfaces 2014, 6, 9118−9125

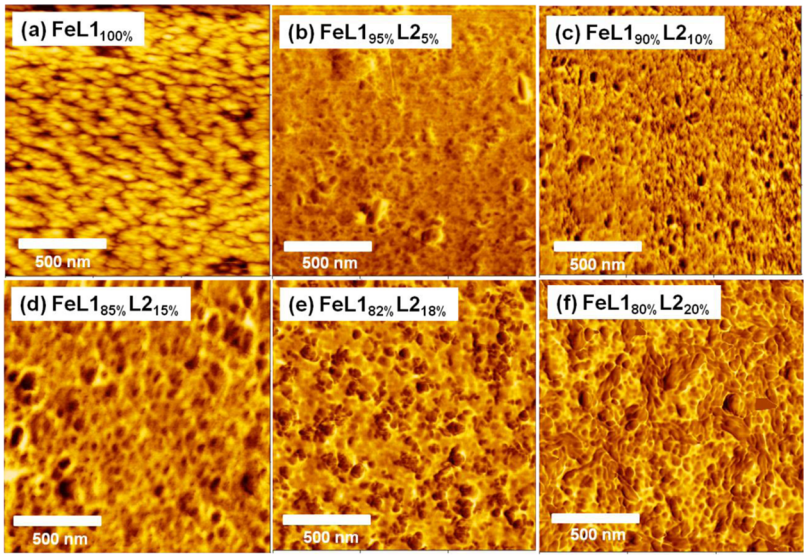

Figure 1. AFM images of the (a) 1-D and (b–f) 3-D Fe(II)-based metallo-supramolecular polymers with different molar ratios of **L1** and **L2**.

diethyl ether to afford **L2** (532 mg, 53.2%). Melting point >300 °C (lit.: 374 °C).[35] ε_{max}: 297 nm. ^{1}H NMR (300 MHz, $CDCl_3$, TMS): δ 8.84 (s, 6H, tpyH$_{3',5'}$), 8.76 (m, 6H, tpyH$_{3,3''}$), 8.70 (d, 6H, J = 8.1 Hz, tpyH$_{6,6'}$), 8.09 (d, 6H, J = 8.2 Hz, H$_{Ar}$), 7.97 (s, 3H, H$_c$), 7.92 (d, 6H, J = 8.1 Hz, H$_{Ar}$), 7.90 (m, 6H, tpyH$_{4,4''}$), 7.37 (m, 6H, tpyH$_{5,5''}$). MALDI-TOF-MS: m/z (%) = 999 (100) [M + H].

Synthesis of FeL1$_{100\%}$. **FeL1$_{100\%}$** was obtained according to the literature.[13] An equimolar amount of **L1** and Fe(OAc)$_2$ was refluxed in argon-saturated CH_3COOH (ca. 10 mL of solvent per milligram of **L1**) for 24 h. The reaction solution was cooled to room temperature and then filtered to remove a very small amount of insoluble residues. The filtrate was placed in a Petri dish and the solvent evaporated slowly to dryness. The brittle film was collected and dried further under vacuum overnight to give the corresponding **FeL1$_{100\%}$** (>92%).

Synthesis of FeL1$_{x\%}$L2$_{y\%}$. Different molar ratios of **L1** and **L2** were used for the synthesis of **FeL1$_{x\%}$L2$_{y\%}$** (Table S1, Supporting Information). First, equimolar amounts of **L1** and Fe(OAc)$_2$ were added to argon-saturated absolute acetic acid and stirred at 70 °C for 16 h to synthesize the linear polymer. Then, the calculated amount of **L2** was dissolved in chloroform in advance and then added into the reaction mixture. Fe(OAc)$_2$ (the equimolar amount of **L2**) was also added to the flask and the reaction mixture was stirred for another 24 h. Following the same purification method used for **FeL1$_{100\%}$**, **FeL1$_{x\%}$L2$_{y\%}$** was obtained with >90% yield.

Sample Preparations. (a) Atomic force microscopy (AFM) samples: A fixed amount (100 μL) of the polymer solution (0.5 mg mL^{-1} in methanol) was dripped on a glass slide and dried at room temperature for 1 day. (b) For AFM measurements, we used NanoNavi II of Seiko Instruments Inc. (SII) in dynamic force mode (DFM). We used microcantilevers (Seiko Instruments Inc., Japan) with tips of type SI-DF40 (C = 31 N/m, and f_0 = 307 kHz). The AFM was operated in contact mode in air by silicon cantilevers with spring constants of 0.01–0.5 N/m. The image scan size was between 1.5 × 1.5 μm with a scan speed of 1.00 Hz. (c) CV measurements: all the polymer films were prepared on an indium tin oxide (ITO) glass (8–12 Ω/sq, 25 × 25 × 1.1 mm, Sigma-Aldrich) with a fixed working area of 1.0 × 1.5 cm by the spray-coating method. Each film had the same absorbance at its own MLCT band with an error bar of 0.05.

RESULTS AND DISCUSSION

Surface Morphology of the 3-D Metallo-Supramolecular Polymers. For the atomic force microscopy (AFM) measurements, the polymer films were prepared by drop-coating the polymer solutions onto a glass slide. The surface of the **FeL1$_{100\%}$** film was discontinuous and had a cotton-like apparent (Figure 1a). The root-mean-square roughness (R_{rms}) measured from the image was small (2.9 nm). In the **FeL1$_{95\%}$L2$_{5\%}$** film, the discontinuous surface was flatter with small hills, but the cotton-like structures still existed (R_{rms}: ca. 3.5 nm) (Figure 1b). It is considered that **L2** acted as a simple "linker" between the 1-D polymer chains in **FeL1$_{95\%}$L2$_{5\%}$**. However, a dramatic morphology change was observed in **FeL1$_{90\%}$L2$_{10\%}$** and **FeL1$_{85\%}$L2$_{15\%}$** (Figures 1c,d); many holes approximately 30–50 nm in diameter appeared on the surface and the number of holes increased with increasing ratio of **L2**. The R_{rms} increased to 5.8 nm in **FeL1$_{90\%}$L2$_{10\%}$**. The surface of the **FeL1$_{85\%}$L2$_{15\%}$** film showed a highly porous 3-D structure, probably due to the formation of hyperbranched polymer chains, and the R_{rms} reached 6.0 nm. The literature[31] has reported AFM images of cross-linked supramolecular polymer films with molar ratios of linear/branched ligands of 97/3 and 91/9, but they did not show a hyperbranched or cross-linked structure, probably because the synthesis method of the current 3-D polymer is different and the tritopic ligand **L2** is more rigid than the ligand used in the literature. In **FeL1$_{82\%}$L2$_{18\%}$** and **FeL1$_{80\%}$L2$_{20\%}$**, the large holes and porous structure disappeared and the film surfaces became rigid and solid (Figures 1e,f). At the same time, the R_{rms} values decreased to 3.4 and 3.8 nm, respectively.

The morphology change is explained as follows. In **FeL1$_{95\%}$L2$_{5\%}$**, the small amount of **L2** simply links the 1-D polymer chains (Figure 2a). In **FeL1$_{90\%}$L2$_{10\%}$** and

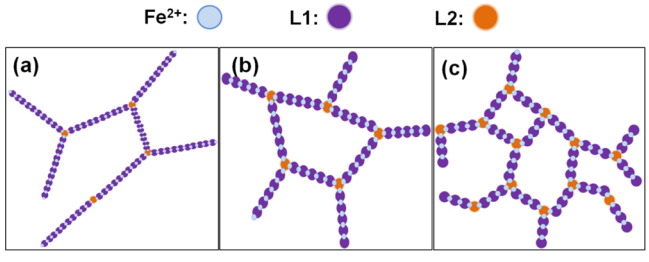

Figure 2. Anticipated polymer structures in (a) **FeL1$_{95\%}$L2$_{5\%}$**, (b) **FeL1$_{90\%}$L2$_{10\%}$** and **FeL1$_{85\%}$L2$_{15\%}$**, and (c) **FeL1$_{82\%}$L2$_{18\%}$** and **FeL1$_{80\%}$L2$_{20\%}$**.

dx.doi.org/10.1021/am5010859 | ACS Appl. Mater. Interfaces 2014, 6, 9118–9125

FeL1$_{85\%}$L2$_{15\%}$, **L2** not only connects the 1-D polymer chains but also forms a hyperbranched polymeric structure, which results in the porous surface (Figure 2b). However, when the ratio of **L2** higher than 15% (**FeL1$_{82\%}$L2$_{18\%}$** and **FeL1$_{80\%}$L2$_{20\%}$**), the expanded hyperbranched structure made the polymer film rigid and insoluble (Figure 2c).

UV–Vis Spectroscopy and Cyclic Voltammetry. In the UV–vis spectra of the polymer solutions (solvent, MeOH; concentration, 50 μM), the maximum wavelength (λ_{max}) in the MLCT absorption was progressively blue-shifted with increasing **L2** ratio (**FeL1$_{100\%}$**, 585.2 nm; **FeL1$_{80\%}$L2$_{20\%}$**, 578.7 nm) (Figure 3). The blue shift indicates that the lowest unoccupied

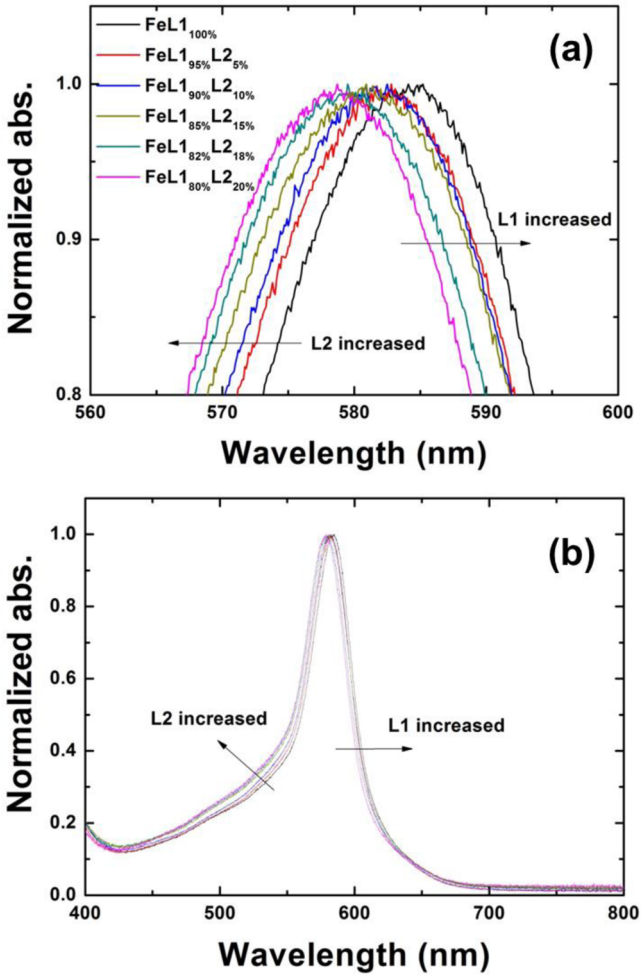

Figure 3. UV–vis spectra of the 3-D Fe(II)-based metallo-supramolecular polymers in the (a) 560–600 nm and (b) 400–800 nm regions.

molecular orbital (LUMO) potential of the ligand in the MLCT absorption increased. The π-conjugation in **L2** is shorter than that in **L1** because the three terpyridine moieties of **L2** are connected at the (non-conjugated) meta position of the central phenyl ring. Therefore, it is reasonable that the less π-conjugated **L2** enhanced the LUMO potential of the MLCT absorption in the complex. The CV of the polymer films showed only a small difference in the anodic peak potential (E_{pa}) (Figure 4). To confirm the redox peak position precisely, polymer films with the same thickness and same active area were used and a very slow scan rate (10 mV s^{-1}) was applied. The 3-D structure did not significantly affect the redox

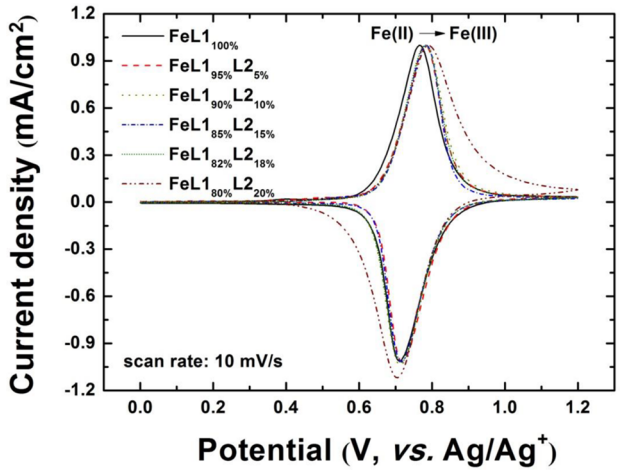

Figure 4. Cyclic voltammograms of the 3-D polymers (electrolyte, 0.1 M $LiClO_4$; ACN scan rate, 10 mV s^{-1}).

potential, but slightly increased resistance as a result of cross-linking is suggested by the increased redox peak separation and larger reaction area in **FeL1$_{80\%}$L2$_{20\%}$** film. This result indicates that ionic exchange in the polymer film decreased when the **L2** ratio exceeded 18%.

Thermal Analysis and Solubility. Thermogravimetric analysis (TGA) showed that the 3-D structure enhanced the thermal stability of the polymer films, probably because of the cross-linking. The temperature for a 5% weight loss (T_d) in **FeL1$_{100\%}$** was 367.9 °C, and significant weight loss was observed at temperatures higher than 370 °C (Figure 5), whereas the weight decreased quite slowly up to 450 °C in the 3-D polymers. All the data are summarized in Table 1.

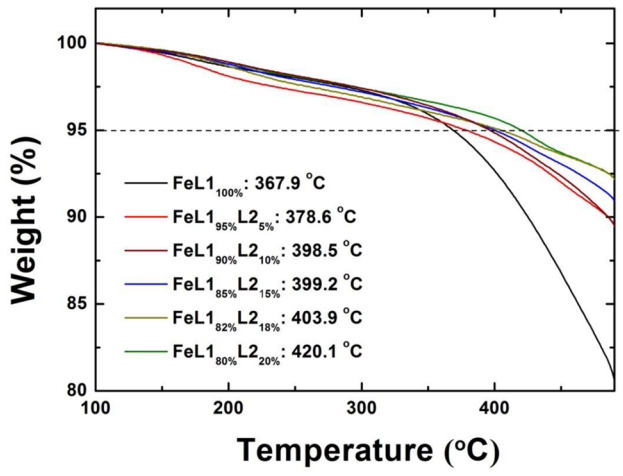

Figure 5. Thermogravimetric analysis of the 3-D polymers. The temperature was increased from room temperature to 500 °C at a rate of 10 °C min^{-1}.

The obtained polymers have good solubility in methanol. In the case of polymers with a π-conjugated structure, the solubility is often decreased by the strong stacking among the polymer chains. However, the hyperbranched, rigid structure of π-conjugated polymers does not always decrease the solubility of the polymer, because the hyperbranched structure prevents the stacking of polymer chains. For example, dendritic π-

dx.doi.org/10.1021/am5010859 | ACS Appl. Mater. Interfaces 2014, 6, 9118–9125

Table 1. Optical and Electrochemical Properties: Maximum Wavelength of the MLCT Absorption (λ_{max}), the Anodic Peak Potential (E_{pa}), the Peak Separation in the Redox (ΔE), the Thermal Stability (T_d), and the Solubility of the Polymer Films

3-D or 1-D polymers	λ_{max} [nm][a]	E_{pa} [mV][b]	ΔE [V][c]	T_d [°C][d]	solubility[e]
FeL1$_{100\%}$	585.2	0.765	0.055	367.9	+++
FeL1$_{95\%}$L2$_{5\%}$	582.8	0.780	0.065	378.6	+++
FeL1$_{90\%}$L2$_{10\%}$	582.5	0.780	0.065	398.5	+++
FeL1$_{85\%}$L2$_{15\%}$	580.2	0.785	0.070	399.2	++
FeL1$_{82\%}$L2$_{18\%}$	579.5	0.790	0.080	403.9	+
FeL1$_{80\%}$L2$_{20\%}$	578.7	0.795	0.090	420.1	+

[a]The polymer films were prepared by spray coating a 1 mg mL^{-1} methanol solution of the polymer onto an ITO glass (working area: 1 × 1.5 cm). All the polymer films had the same thickness of approximately 500 ± 34 nm, which was estimated using a surface profiler (Alpha-step IQ, KLA Tencor). [b]The polymer films used in the UV−vis spectral measurements were also used for the cyclic voltammetry measurements (electrolyte: an ACN solution of 0.1 M $LiClO_4$; counter electrode: platinum wire; reference electrode: Ag/Ag$^+$; scan rate: 10 mV s^{-1}) at room temperature. [c]The differences in the redox potentials ($E_{ox} - E_{red}$). [d]The temperature for the 5% weight loss in the thermogravimetric analysis (TGA) (the temperature increase rate: 10 °C min^{-1}). [e]The solubility was examined by dissolving 1 mg of the polymer into 1 mL of methanol. The symbol "+++" means the polymer was totally dissolved in methanol and there was no precipitation after 72 h. The symbol "++" means the polymer was totally dissolved in methanol but precipitation happened within 72 h. The symbol "+" means the polymer was partially dissolved in methanol.

conjugated polymers and the macromolecular metal complexes have high solubility.[36,37]

Electron Transfer Mechanism in 3-D Film. The electron transfer mechanism can be investigated by the current measurement in redox peaks of the CV with the different scan rates. For example, if anodic peak current (i_{pa}) is proportional to scan rate (υ), the rate-determining step in the redox reaction is on the electron transfer on the electrode.[38] On the other hand, when i_{pa} is proportional to $\upsilon^{1/2}$, the rate-determining step is on the diffusion speed of the electroactive species or ionic groups to the electrode.[39] The CVs of **FeL1$_{100\%}$** and **FeL1$_{85\%}$L2$_{15\%}$** films with the same thickness were measured with different scan rates (Figure 6a,d). In the plots of the observed current as a function of the scan rate and the square root of the scan rate in the **FeL1$_{100\%}$** film, the minimum mean square errors (R^2) were close to 1.0 (Figure 6b,c), which shows that the redox reaction follows both kinetic control and diffusion control equally. This means that the electron transfer rate is almost the same as the diffusion rate of the counter anions during the redox. On the other hand, the redox in the 3-D **FeL1$_{85\%}$L2$_{15\%}$** film was clearly diffusion-controlled, which is supported by the linear relationship between the current and the square root of the scan rate (Figure 6e,f). This result indicates that the diffusion of the counter anion became a rate-determining step as a result of faster electron transfer in the 3-D polymer film than in the 1-D polymer film. The EC properties of the 3-D polymers are presented in Table 2.

Electrochromic Properties. The transmittance change (ΔT) at 580 nm in the **FeL1$_{85\%}$L2$_{15\%}$** film was determined from the difference of the transmittances at 0 and 1.2 V (interval time: 5 s) (Figure 7a). To avoid the effect of the film thickness on ΔT, each film was prepared by a spray-coating method in which the spray conditions were controlled so that all the films had the same absorbance in the MLCT band before immersion into the electrolyte. It was revealed that the 3-D polymers showed higher ΔT than the 1-D polymer except for

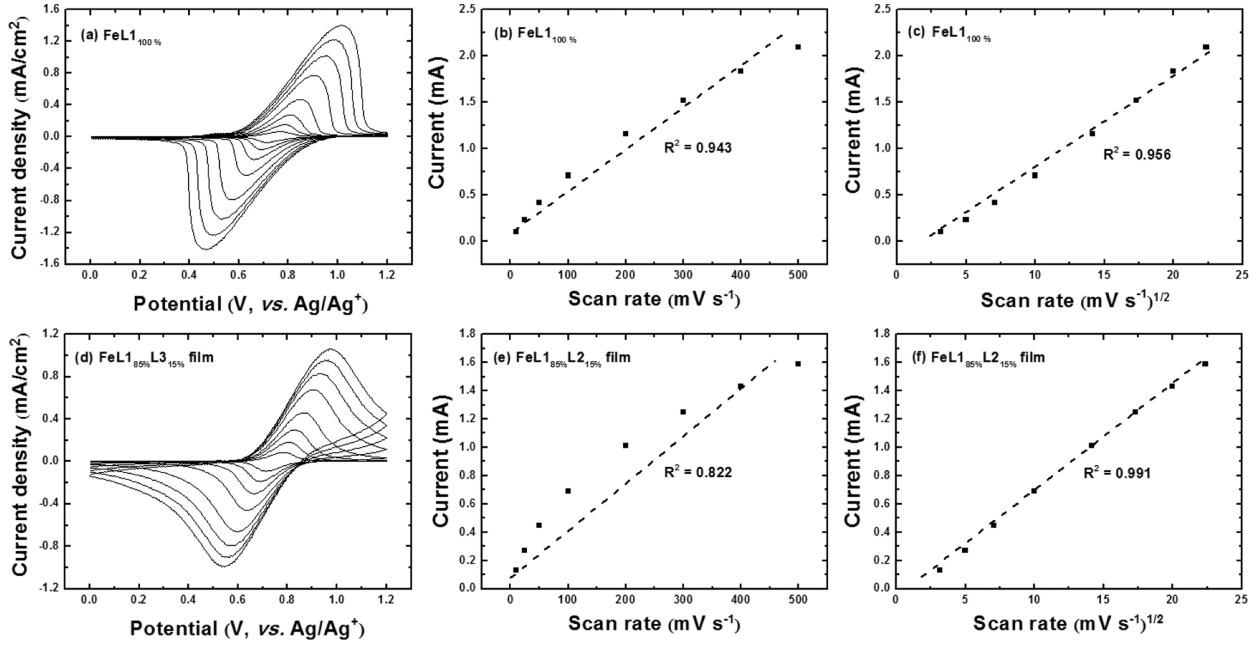

Figure 6. (a) CV of **FeL1$_{100\%}$** with different scan rates (10−500 mV/s) in a 0.1 M $LiClO_4$/ACN electrolyte. (b) Increase of the peak current in the oxidation of the Fe^{2+} ions as a function of the increased scan rate in the **FeL1$_{100\%}$** film. (c) Increase of the peak current in the oxidation of the Fe^{2+} ions and the square root of the scan rate in the **FeL1$_{100\%}$** film. (d) CV of **FeL1$_{85\%}$L2$_{15\%}$** films with different scan rates (10−500 mV/s) in a 0.1 M $LiClO_4$/ACN electrolyte. (e) Increase of the peak current in the oxidation of the Fe^{2+} ions as a function of the increased scan rate in the **FeL1$_{85\%}$L2$_{15\%}$** film. (f) Increase of the peak current in the oxidation of the Fe^{2+} ions and the square root of the scan rate in the **FeL1$_{85\%}$L2$_{15\%}$** film.

dx.doi.org/10.1021/am5010859 | ACS Appl. Mater. Interfaces 2014, 6, 9118−9125

Table 2. EC Properties: Transmittance in the Bleached and Colored States, Transmittance Contrast (ΔT), Switching Time, Charge/Discharge Ratios, And Coloration Efficiencies (η) of the Polymer Films

3-D or 1-D polymers	$T_{bleached}$ [%][a]	$T_{colored}$ [%][a]	ΔT [%][a]	$t_{coloring}$ [s][b]	$t_{bleaching}$ [s][b]	charge/discharge [mC][c]	η [cm^2/C][d]
FeL1$_{100\%}$	93.2	51.6	41.6	0.31	0.58	1.46/1.44	263.8
FeL1$_{95\%}$L2$_{5\%}$	92.5	43.9	48.6	0.21	0.51	1.69/1.65	287.2
FeL1$_{90\%}$L2$_{10\%}$	94.0	46.5	47.5	0.23	0.52	1.38/1.35	332.2
FeL1$_{85\%}$L2$_{15\%}$	91.6	40.9	50.7	0.19	0.36	1.37/1.34	383.4
FeL1$_{82\%}$L2$_{18\%}$	78.8	54.8	24.0	0.37	0.60	1.69/1.65	140.0
FeL1$_{80\%}$L2$_{20\%}$	81.6	54.4	27.2	0.37	0.62	2.02/1.97	130.7

All the values of the electrochromic properties, including transmittance ($T_{bleached}$ and $T_{colored}$), transmittance change (ΔT), switching time ($t_{coloring}$ and $t_{bleaching}$), and coloration efficiency (η), were averaged from three data points of our polymer films. The errors of these values were less than ±5%. [a]The transmittances of the MLCT absorption (λ_{max}) in the bleached ($T_{bleached}$) and colored states ($T_{colored}$) of the polymer film coated on an ITO glass were measured by *in-situ* UV-vis spectroscopy at 0 or 1.2 V *vs.* Ag/Ag$^+$ with an interval time of 5 s (electrolyte: 0.1 M $LiClO_4$/ACN; the ITO working area: 1 × 1.5 cm). The transmittance difference (ΔT) was calculated from $T_{bleached}$ and $T_{colored}$. [b]The times for coloring and bleaching ($t_{coloring}$ and $t_{bleaching}$) were defined as the time taken for 95% of ΔT to change. [c]The charge/discharge values were calculated from the integration of the coulomb number in the current response during the redox. [d]The coloration efficiency (η) was defined as the relationship between the electron charge used and the change of ΔT.

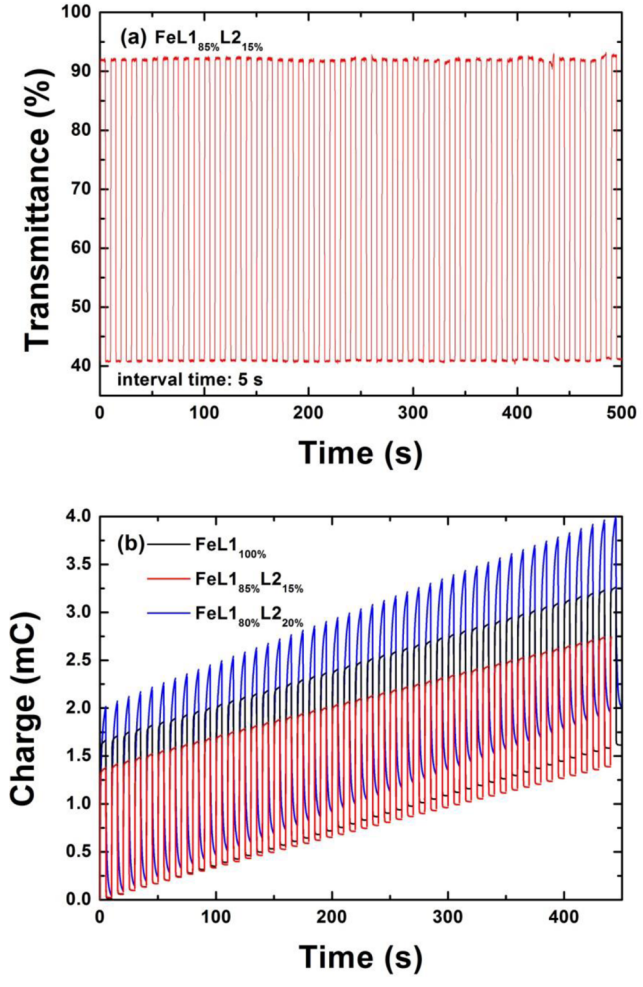

Figure 7. (a) Transmittance change (ΔT, %) of the **FeL1$_{85\%}$L2$_{15\%}$** film at 580 nm during voltage switching between 0 and 1.2 V (interval: 5 s) in 0.1 M $LiClO_4$/ACN. (b) Change of charge in the **FeL1$_{100\%}$**, **FeL1$_{85\%}$L2$_{15\%}$**, and **FeL1$_{80\%}$L2$_{20\%}$** films during switching between 0 and 1.2 V. The larger slope of **FeL1$_{80\%}$L2$_{20\%}$** means more electron loss during voltage switching; the slopes of the three lines can also indicate the charge resistance in polymer films. The change of charge shows how much charge is used in switching: the smaller the charge used, the higher the obtained coloration efficiency.

FeL1$_{82\%}$L2$_{18\%}$ and **FeL1$_{80\%}$L2$_{20\%}$**. Additionally, except for the above-mentioned two polymer films, the switching time ($t_{coloring}$ and $t_{bleaching}$) in the 3-D polymer films was faster than that in the 1-D linear **FeL1$_{100\%}$** film. The overly cross-linked films showed a slower response and a smaller ΔT; the more the electron charge used, the worse the coloration efficiency (η).

Coloration efficiency, η, is a useful parameter for determining the quality of ECMs. The relationship between the optical density change (ΔOD) and the injected/ejected electronic charge (Q_d) is given by the following equation:[40−42]

$$\eta = \frac{\Delta \mathrm{OD}}{Q_d} = \log \frac{T_b}{T_c} / Q_d \quad (1)$$

A high η value is obtained when the ECMs have a large optical change and/or low electronic charge. Figure 7b shows the electron charge/discharge behaviors of the **FeL1$_{100\%}$**, **FeL1$_{85\%}$L2$_{15\%}$**, and **FeL1$_{80\%}$L2$_{20\%}$** films (interval time, 5 s; applied voltages, 0 and 1.2 V). The slopes show electrochemical reversibility in the EC change: the large slope means the charge and discharge amounts are not the same. The **FeL1$_{100\%}$** and **FeL1$_{85\%}$L2$_{15\%}$** films have almost the same slope (charge/discharge ratios), but the 3-D polymer film used less charge and obtained a higher optical change (ΔT), resulting in better η. The **FeL1$_{80\%}$L2$_{20\%}$** film used more charge in color switching but obtained less ΔT, meaning that the electron transfer efficiency in the overly cross-linked structure was quite low and caused more charge waste in the cross-linked film. From eq 1, we know that the more charge that is used in the film, the lower the η obtained. We compared the 1-D linear **FeL1$_{100\%}$** and the well-cross-linked **FeL1$_{85\%}$L2$_{15\%}$** films. The response time was improved 38.7% for the coloring (0.31 → 0.19 s) and 37.9% for the bleaching (0.58 → 0.36 s). ΔT increased 21.8% (41.6 → 50.7%), and η was also enhanced 45.3% (263.8 → 383.4 cm^2 C^{-1}).

CONCLUSIONS

A series of Fe(II)-based metallo-supramolecular polymers with a 3-D structure were successfully synthesized using a tris-(terpyridine) ligand **L2** as the cross-linker. By changing the molar ratio of **L1** and **L2**, significantly different surface morphologies and EC properties were observed. An **FeL1$_{85\%}$L2$_{15\%}$** film with a highly porous surface (pore size: approximately 30−50 nm in diameter) showed the best EC properties among the 3-D and 1-D polymers (response time for

the coloring, 0.19 s; response time for the bleaching, 0.36 s; ΔT, 50.7%; η, 383.4 $cm^2\ C^{-1}$), probably because of the smooth anion transfer inside the porous polymer film. In addition, this method of changing the film morphology will be useful for improving the electrochromic properties of the other metallo-supramolecular polymers.

■ ASSOCIATED CONTENT

Supporting Information

^{1}H NMR and MALDI-TOF-MS spectra of **L2**, transmittance change (ΔT, %) at the λ_{max} in **FeL1**$_{x\%}$**L2**$_{y\%}$ films, and the feed molar ratios of **L1**, **L2** and Fe(II) in the metallo-supramolecular polymers. This material is available free of charge via the Internet at http://pubs.acs.org.

■ AUTHOR INFORMATION

Corresponding Author

*Masayoshi Higuchi. E-mail: HIGUCHI.Masayoshi@nims.go.jp. Tel&Fax: +81-29-860-4721.

Notes

The authors declare no competing financial interest.

■ ACKNOWLEDGMENTS

This work is financially supported by CREST project toward "Electrochromic Color-E-Paper" in Japan Science and Technology Agency (JST).

■ REFERENCES

(1) Deb, S. K. A Novel Electrophotographic System. *Appl. Opt. Suppl.* **1969**, *3*, 192−195.
(2) Schoot, C. J.; Ponjee, J. J.; Vandam, H. T.; Vandoorn, R. A.; Bolwijn, P. T. New Electrochromic Memory Display. *Appl. Phys. Lett.* **1973**, *23*, 64−65.
(3) Reichman, B.; Bard, A. J. The Electrochromic Process at WO_3 Electrodes Prepared by Vacuum Evaporation and Anodic Oxidation of W. *J. Electrochem. Soc.* **1979**, *126*, 583−591.
(4) Itaya, K.; Shibayama, K.; Akahoshi, H.; Toshima, S. Prussian-Blue-Modified Electrodes—An Application for a Stable Electrochromic Display Device. *J. Appl. Phys.* **1982**, *53*, 804−805.
(5) Honda, K.; Fujita, M.; Ishida, H.; Yamamoto, R.; Ohgaki, K. Solid-State Electrochromic Devices Composed of Prussian Blue, WO_3, and Poly(ethylene oxide)-Polysiloxane Hybrid-Type Ionic Conducting Membrane. *J. Electrochem. Soc.* **1988**, *135*, 3151−3154.
(6) Jiang, M.; Zhao, Z. F. A Novel Stable Electrochromic Thin-Film - A Prussian Blue Analog Based on Palladium Hexacyanoferrate. *J. Electroanal. Chem.* **1990**, *292*, 281−287.
(7) Toshima, N.; Lin, R. J.; Kaneko, M. A New Preparation Method of Electrochromic Prussian Blue Films by Casting a Solution and Their Electrochemical Properties. *Chem. Lett.* **1990**, 485−488.
(8) Shirota, Y. Organic Materials for Electronic and Optoelectronic Devices. *J. Mater. Chem.* **2000**, *10*, 1−25.
(9) Heuer, H. W.; Wehrmann, R.; Kirchmeyer, S. Electrochromic Window Based on Conducting Poly (3,4-ethylenedioxythiophene)-poly(styrene sulfonate). *Adv. Funct. Mater.* **2002**, *12*, 89−94.
(10) Mortimer, R. J.; Dyer, A. L.; Reynolds, J. R. Electrochromic Organic and Polymeric Materials for Display Applications. *Displays* **2006**, *27*, 2−18.
(11) Beaujuge, P. M.; Reynolds, J. R. Color Control in pi-Conjugated Organic Polymers for Use in Electrochromic Devices. *Chem. Rev.* **2010**, *110*, 268−320.
(12) Han, F. S.; Higuchi, M.; Kurth, D. G. Metallo-Supramolecular Polymers Based on Functionalized Bis-terpyridines as Novel Electrochromic Materials. *Adv. Mater.* **2007**, *19*, 3928−3931.
(13) Higuchi, M.; Kurth, D. G. Electrochemical Functions of Metallosupramolecular Nanomaterials. *Chem. Rec.* **2007**, *7*, 203−209.
(14) Han, F. S.; Higuchi, M.; Akasaka, Y.; Otsuka, Y.; Kurth, D. G. Preparation, Characterization, and Electrochromic Properties of Novel Co(II)-Bis-2,2′:6′,2″-Terpyridine Metallo-Supramolecular Polymers. *Thin Solid Films* **2008**, *516*, 2469−2473.
(15) Kurth, D. G. Metallo-Supramolecular Modules as a Paradigm for Materials Science. *Sci. Technol. Adv. Mater.* **2008**, *9*, 014103.
(16) Higuchi, M. Electrochromic Functions of Organic-Metallic Hybrid Polymers. *J. Nanosci. Nanotechnol.* **2009**, *9*, 51−58.
(17) Higuchi, M. Electrochromic Organic-Metallic Hybrid Polymers: Fundamentals and Device Applications. *Polym. J.* **2009**, *41*, 511−520.
(18) Tieke, B. Coordinative Supramolecular Assembly of Electrochromic Thin Films. *Curr. Opin. Colloid Interface Sci.* **2011**, *16*, 499−507.
(19) Han, F. S.; Higuchi, M.; Kurth, D. G. Metallosupramolecular Polyelectrolytes Self-Assembled from Various Pyridine Ring-Substituted Bisterpyridines and Metal Ions: Photophysical, Electrochemical, and Electrochromic Properties. *J. Am. Chem. Soc.* **2008**, *130*, 2073−2081.
(20) Hossain, M. D.; Sato, T.; Higuchi, M. A Green Copper-Based Metallo-Supramolecular Polymer: Synthesis, Structure, and Electrochromic Properties. *Chem.—Asian J.* **2013**, *8*, 76−79.
(21) Hu, C.-W.; Sato, T.; Zhang, J.; Moriyama, S.; Higuchi, M. Multi-Colour Electrochromic Properties of Fe/Ru-Based Bimetallo-Supramolecular Polymers. *J. Mater. Chem. C* **2013**, *1*, 3408−3413.
(22) Yoo, S. J.; Lim, J. W.; Sung, Y. E.; Jung, Y. H.; Choi, H. G.; Kim, D. K. Fast Switchable Electrochromic Properties of Tungsten Oxide Nanowire Bundles. *Appl. Phys. Lett.* **2007**, *90*, 173126.
(23) Chen, D. L.; Gao, L.; Yasumori, A.; Kuroda, K.; Sugahara, Y. Size- and Shape-Controlled Conversion of Tungstate-Based Inorganic-Organic Hybrid Belts to WO_3 Nanoplates with High Specific Surface Areas. *Small* **2008**, *4*, 1813−1822.
(24) Long, Y. Z.; Li, M. M.; Gu, C. Z.; Wan, M. X.; Duvail, J. L.; Liu, Z. W.; Fan, Z. Y. Recent Advances in Synthesis, Physical Properties and Applications of Conducting Polymer Nanotubes and Nanofibers. *Prog. Polym. Sci.* **2011**, *36*, 1415−1442.
(25) Wei, H. Y.; Hsiao, Y. S.; Huang, J. H.; Hsu, C. Y.; Chang, F. C.; Chen, P. L.; Ho, K. C.; Chu, C. W. Dual-Color Electrochromic Films Incorporating a Periodic Polymer Nanostructure. *RSC Adv.* **2012**, *2*, 4746−4753.
(26) Wang, J. P.; Zhang, D. H. One-Dimensional Nanostructured Polyaniline: Syntheses, Morphology Controlling, Formation Mechanisms, New Features, and Applications. *Adv. Polym. Technol.* **2013**, *32*, E323−E368.
(27) Gasnier, A.; Royal, G.; Terech, P. Metallo-Supramolecular Gels Based on a Multitopic Cyclam Bis-Terpyridine Platform. *Langmuir* **2009**, *25*, 8751−8762.
(28) Higuchi, M.; Akasaka, Y.; Ikeda, T.; Hayashi, A.; Kurth, D. G. Electrochromic Solid-State Devices Using Organic-Metallic Hybrid Polymers. *J. Inorg. Organomet. Polym. Mater.* **2009**, *19*, 74−78.
(29) da Silva, C. A.; Vidotti, M.; Fiorito, P. A.; de Torresi, S. I. C.; Torresi, R. M.; Alves, W. A. Electrochromic Properties of a Metallo-supramolecular Polymer Derived from Tetra(2-pyridyl-1,4-pyrazine) Ligands Integrated in Thin Multilayer Films. *Langmuir* **2012**, *28*, 3332−3337.
(30) Hossain, M. D.; Higuchi, M. Synthesis of Metallo-Supramolecular Polymers Using 5,5′-Linked Bis(1,10-Phenanthroline) Ligands. *Synthesis* **2013**, *45*, 753−758.
(31) Sievers, T. K.; Vergin, A.; Mohwald, H.; Kurth, D. G. Thin Films of Cross-Linked Metallo-Supramolecular Coordination Polyelectrolytes. *Langmuir* **2007**, *23*, 12179−12184.
(32) Maier, A.; Rabindranath, R.; Tieke, B. Fast-Switching Electrochromic Films of Zinc Polyiminofluorene-Terpyridine Prepared Upon Coordinative Supramolecular Assembly. *Adv. Mater.* **2009**, *21*, 959−963.
(33) Maier, A.; Cheng, K. L.; Savych, J.; Tieke, B. Double-Electrochromic Coordination Polymer Network Films. *ACS Appl. Mater. Interfaces* **2011**, *3*, 2710−2718.
(34) Welterlich, I.; Tieke, B. Conjugated Polymer with Benzimidazolylpyridine Ligands in the Side Chain: Metal Ion Coordination and

Coordinative Self-Assembly into Fluorescent Ultrathin Films. *Macromolecules* **2011**, *44*, 4194−4203.
(35) Cavazzini, M.; Quici, S.; Scalera, C.; Puntoriero, F.; La Ganga, G.; Campagna, S. Synthesis, Characterization, Absorption Spectra, and Luminescence Properties of Multinuclear Species Made of Ru(II) and Ir(III) Chromophores. *Inorg. Chem.* **2009**, *48*, 8578−8592.
(36) Higuchi, M.; Shiki, S.; Ariga, K.; Yamamoto, K. First Synthesis of Phenylazomethine Dendrimer Ligands and Structural Studies. *J. Am. Chem. Soc.* **2001**, *123*, 4414−4420.
(37) Yamamoto, K.; Higuchi, M.; Shiki, S.; Tsuruta, M.; Chiba, H. Stepwise Radial Complexation of Imine Groups in Phenylazomethine Dendrimers. *Nature* **2002**, *415*, 509−511.
(38) Wang, C.; Yang, C.; Song, Y.; Gao, W.; Xia, X. Adsorption and Direct Electron Transfer from Hemoglobin into a Three-Dimensionally Ordered Macroporous Gold Film. *Adv. Funct. Mater.* **2005**, *15*, 1267−1275.
(39) Kissinger, P. T.; Heineman, W. R. Cyclic Voltammetry. *J. Chem. Educ.* **1983**, *60*, 702−706.
(40) Sapp, S. A.; Sotzing, G. A.; Reynolds, J. R. High Contrast Ratio and Fast-Switching Dual Polymer Electrochromic Devices. *Chem. Mater.* **1998**, *10*, 2101−2108.
(41) Argun, A. A.; Aubert, P. H.; Thompson, B. C.; Schwendeman, I.; Gaupp, C. L.; Hwang, J.; Pinto, N. J.; Tanner, D. B.; MacDiarmid, A. G.; Reynolds, J. R. Multicolored Electrochromism Polymers: Structures and Devices. *Chem. Mater.* **2004**, *16*, 4401−4412.
(42) Deb, S. K. Opportunities and Challenges in Science and Technology of WO_3 for Electrochromic and Related Applications. *Sol. Energy Mater. Sol. Cells* **2008**, *92*, 245−258.